



UNIVERSITY OF LEEDS

This is a repository copy of *Preparation and Evaluation of CaO-Based CO₂ Sorbents Deposited on Saffil Fiber Supports*.

White Rose Research Online URL for this paper:

<https://eprints.whiterose.ac.uk/133434/>

Version: Accepted Version

Article:

Ramirez Solis, S orcid.org/0000-0003-1951-0724, Dupont, V orcid.org/0000-0002-3750-0266 and Milne, SJ orcid.org/0000-0002-1365-7365 (2018) Preparation and Evaluation of CaO-Based CO₂ Sorbents Deposited on Saffil Fiber Supports. *Energy & Fuels*, 32 (8). pp. 8631-8640. ISSN 0887-0624

<https://doi.org/10.1021/acs.energyfuels.8b00986>

© 2018 American Chemical Society. This is an author produced version of a paper published in *Energy & Fuels*. Uploaded in accordance with the publisher's self-archiving policy.

Reuse

Items deposited in White Rose Research Online are protected by copyright, with all rights reserved unless indicated otherwise. They may be downloaded and/or printed for private study, or other acts as permitted by national copyright laws. The publisher or other rights holders may allow further reproduction and re-use of the full text version. This is indicated by the licence information on the White Rose Research Online record for the item.

Takedown

If you consider content in White Rose Research Online to be in breach of UK law, please notify us by emailing eprints@whiterose.ac.uk including the URL of the record and the reason for the withdrawal request.



eprints@whiterose.ac.uk
<https://eprints.whiterose.ac.uk/>

Preparation and Evaluation of CaO-based CO₂ Sorbents Deposited on Saffil Fibre Supports

Sergio Ramirez-Solis, Valerie Dupont, Steven J. Milne*

School of Chemical and Process Engineering (SCAPE), University of Leeds, Leeds LS2 9JT, UK.

Abstract

Calcium oxide-based sorbents were coated onto Saffil ceramic fibres by means of a wet impregnation method. The effect of synthesis parameters on the crystalline structure, morphology and texture of the CaO layer were investigated by X-ray diffraction, scanning electron microscopy and gas adsorption techniques. The analyses revealed that the optimised synthesis method produced a uniform coating composed of a network of CaO nanoflakes. The evaluation of the materials as CO₂ sorbents was performed under repeated carbonation-decarbonation cycles using thermogravimetric analysis (TGA). A nominal 25 wt. % loading of CaO gave a CO₂ uptake capacity of 0.118 mg CO₂/mg of sorbent (carbonation at 650°C in 90% CO₂ and decarbonation at 850°C in N₂). A 5 wt. % loading exhibited improved durability with a ~30% decay in carrying capacity after 30 TGA cycles, but at the expense of initial uptake capacity.

Keywords: CO₂ capture materials; CO₂ sorbents; CaO: thermogravimetric analysis; multicycle durability;

1. Introduction

Carbon capture and storage (CCS) has emerged as a promising approach for reducing anthropogenic CO₂ emissions into the atmosphere ^{1, 2}. An estimation demonstrates that CCS technologies could be able to mitigate between 80-90% of the overall CO₂ emitted from combustion carried out in processes such as power plants ^{1, 3}. There are three classes of capture technologies, namely pre-combustion, post-combustion and oxy-combustion ^{4, 5}. In pre-combustion capture, the separation occurs in an exhaust stream derived from a gasification or reforming process prior to the combustion reaction ^{6, 7}, allowing a decarbonised fuel stream to be combusted or oxidised downstream of the CO₂ capture stage. In post-combustion capture, CO₂ is removed from the combustion product stream, commonly composed of N₂, CO₂ and O₂. With respect to oxy-combustion, a special form of post-combustion capture, almost pure oxygen is introduced into the combustion environment rather than air, this results in combustion products devoid of N₂ which allows easy separation of the CO₂ by condensation of the steam co-product ⁸. Although post-combustion capture technologies are considered more mature than pre-combustion systems, the costs can be higher for coal-fired plants ⁶.

Sorption enhanced steam reforming (SESR) as a pre-combustion process is an attractive route to produce high purity H₂ through the separation of CO₂ from the gas phase at high temperature (>400°C). High conversions of methane (CH₄) and CO with no requirement for a purification unit are advantages of the SESR approach. However, the optimisation of this process is intrinsically related to the appropriate selection of CO₂ sorbents, as these

materials must show an ability to withstand harsh operating conditions, with minimal degradation of CO₂ capture performance over multiple high temperature sorption-desorption cycles⁹. SESR applications are the motivation for the present study. Several criteria must be carefully considered in selecting an appropriate high-temperature CO₂ capture material, including their thermodynamic properties and capture capacity within the expected operating temperature and pressure ranges^{10, 11}. Additionally, account must be taken of the kinetics of sorption and desorption and their dependence on textural properties (active surface area and pore volume). For applications at an industrial level, the production costs and the availability of the raw sorbent are also important factors to consider^{12, 13}.

Inorganic sorbents such as CaO, MgO, hydrotalcites (HTC), Li₂ZrO₃ and Li₄SiO₄, have shown promise as high temperature CO₂ capture materials. They have the ability to react chemically with dilute levels of CO₂ in gas streams at temperatures relevant to post combustion capture or SESR through a selective carbonation reaction, and can be regenerated by means of a calcination process^{10, 14, 15}.

Sorbent	Carbonation temperature (°C)	Carbonation pressure (P _{CO₂} -atm)	Calcination temperature (°C)	CO ₂ sorption capacity (g CO ₂ · g ⁻¹ sorbent)	References
Li ₂ ZrO ₃	400-600	1	750-800	~ 0.28	16
Li ₄ SiO ₄	450-700	1	>800	~ 0.36	17
Na ₂ ZrO ₃	700	0.8	900	~ 0.17	18
CaO-Al ₂ O ₃	~650	0.33	>800	~ 0.19	19
CaO/Ca ₁₂ Al ₁₄ O ₃₃	>650	0.2	>850	~ 0.56	20
CaO-MgO	>750	1	>750	~ 0.53	21
CaO-La ₂ O ₃	>650	0.15	>950	~ 0.21	22
CaO-Cs ₂ O	>600	0.29	-	~ 0.66	23
Hydrotalcite (HTC) promoted with K ₂ CO ₃	400-550	0.38	400-550	~ 0.018	24

Table 1. CO₂ uptake capacity for leading metal-oxide sorbent materials tested under different operational conditions of temperature and pressure.

Natural sorbents such as limestone (CaCO_3) and dolomite ($\text{CaMg}(\text{CO}_3)_2$) have been extensively studied for CO_2 removal using batch fluidized bed, fixed bed and dual fluidized bed reactors ^{3, 25}. However, sintering and performance degradation have been encountered. According to numerous publications, the loss of CO_2 reactivity can reach around 80% in the course of carbonation-calcination cycles ^{26, 27}. The drastic decline in the performance of CaO is associated with textural changes such as changes in pore size distribution and reduction in specific surface area. The high temperatures ($>800^\circ\text{C}$) required to regenerate the sorbent encourages a collapse of the pore network and sintering of the powder ^{28, 29}. In order to overcome the detrimental effects caused by sintering of limestone or dolomite derived sorbents, the preparation of synthetic sorbents has been proposed as a viable alternative to enhance and extend the thermal stability and lifetime ^{30, 31}. Their performance depends on the method of synthesis and this offers a means of optimising thermal stability and achieving levels of CO_2 uptake close to the theoretical capacity ³². Table 1 contains a list of some synthetic sorbents which have shown an ability to absorb CO_2 at high temperature. Although they exhibit improved performance with regards to natural materials, there is scope for further improvements in high-temperature multicycle durability.

An extensive range of natural and synthetic solid materials for CO_2 uptake at high temperature have been researched but CaO remains one of the most promising options because of its favourable CO_2 carrying capacity, temperature range of operation, material availability and low production costs ^{33, 34}. Typical carbonation temperatures are between $600\text{-}650^\circ\text{C}$. However, as mentioned above, the main drawback from using CaO as a CO_2 sorbent material is a loss of uptake capacity over repeated use due to densification and loss of porosity and surface area after multiple carbonation-decarbonation cycles due to

the effects of sintering. The rate of sorption slows down due to longer diffusion paths as a result of the sintered dense microstructure ^{30, 35}.

Studies reveal that incorporating CaO into a matrix of a refractory material can enhance multicycle stability. These blends are termed collectively as 'CaO-based sorbents' and include pre-prepared compounds such as $\text{Ca}_{12}\text{Al}_{14}\text{O}_{33}$, CaTiO_3 , CaZrO_3 , and CaO mixed with refractory powders such as MgO, SiO_2 and Al_2O_3 ³⁶⁻³⁸. These improve but do not eliminate loss of performance due to repeated carbonation-calcination cycles. Aluminium oxide powder is regarded as one of the most promising options to stabilise the CaO sorbent against sintering because of its thermal stability (high melting point $>2050^\circ\text{C}$) and robust mechanical properties ^{39, 40}. In addition, Al_2O_3 can be produced with high surface area and a mesoporous structure which is very relevant for a support material ^{41, 42}. The incorporation of CaO and with the Al_2O_3 'spacer' powder is usually performed using wet chemical methods ⁴³.

In the present study, an alternative means of improving the thermal stability of CaO as a CO_2 acceptor is proposed. A low-density fibrous mat of refractory Saffil with outstanding resistance to chemical attack and also to degradation in demanding conditions has been used as a support material on which to deposit CaO with the aim of inhibiting volumetric densification of the active sorbent layer. In addition to prolonging the cyclic reactivity of CaO, the incorporation of Saffil offers the potential to create a composite material which performs well in a fixed-bed reformer. Catalytic grade Saffil fibres are composed of 95-97% Al_2O_3 and 5-3% SiO_2 ; the median fibre diameter is 3-3.5 microns.

2. Materials and methodology

Saffil fibres (catalytic grade) were supplied by Unifrax Limited (UK). The fibres were loaded with various amounts of CaO active phase (5, 15 and 25 wt. %) using a wet impregnation method. The fibrous mat (0.5 g) was added to an aqueous solution of calcium acetate monohydrate ($C_4H_6CaO_4 \cdot H_2O$, ACS reagent $\geq 99.0\%$, Sigma-Aldrich: CaAc) of appropriate concentration. This was heated to 70°C to promote evaporation of the solution over a ~ 4 h period using a hotplate-stirrer. Comparisons of evaporation with or without stirring (500 rpm) were carried out. Afterwards, the fibrous mat of still moist fibres was removed and dried further in a tubular furnace at 120°C overnight. Then, in order to decompose the CaAc phase to CaO, the sample was heated in a tubular furnace at 850°C . Two different calcination times were used, 1 h and 4 h. The prepared sorbents were labelled as 'Ca-Sa-%-WI', where 'Sa' is the abbreviation for Saffil, '%' corresponds to the notional wt. % of CaO (based on proportions of starting reagents) and 'WI' refers to the wet impregnation method.

The morphology of the Saffil-CaO sorbents was examined using scanning electron microscopy (SEM; Hitachi SU8230). The distribution of the active phase over the fibrous support was investigated by energy-dispersive X-ray spectroscopy (Oxford Instruments Aztec Energy EDX system). The textural properties of the Ca-Sa-%-WI sorbents were investigated by gas adsorption. Surface areas were measured using the Brunauer-Emmett-Teller (BET) technique: pore size distributions were measured by means of a Nova 2002 Quantachrome Instrument. Before performing the analysis, the sorbents were degassed under reduced pressure for 3h at 200°C . The pore size distributions were calculated using the method proposed by Barrett-Joyner-Halenda (BJH).

The chemical composition of the as-prepared sorbents was determined through X-ray fluorescence spectroscopy (XRF: Rigaku ZSC Primus II). This enabled the CaO loadings

to be determined accurately. Because of the fibrous nature of the samples a fusion bead method was applied to prepare the XRF samples ⁴⁴. X-ray powder diffraction (XRD) was used for phase analysis (Bruker D8). In order to identify the crystalline phases, the peak positions and intensities were compared to reference patterns from the International Centre for Diffraction Data (ICDD) by means of X'Pert HighScore Plus software (version 4.5).

The CO₂ carrying capacity and multicycle durability of Ca-Sa-%-WI sorbents was assessed by thermogravimetry (Mettler Toledo TGA/DSC1). Initially an isothermal test was conducted for all three sorbent loadings over a 45 min time period ($T_{\text{carbonation}} = 650^{\circ}\text{C}$). The first 'activation' step involved heating to 850°C at 20°C/min under an inert atmosphere (pure N₂). Subsequently, the temperature was lowered to 650°C and then the gas flow was switched to 90% CO₂/10% N₂. After 45 min, the carbonated specimen was subjected to a higher temperature ($T_{\text{decarbonation}} = 850^{\circ}\text{C}$ for 10 min) to decompose the carbonate phase and release the CO₂ previously captured (decarbonation). This process was conducted in flowing N₂. The flow rate applied in the course of the activation, carbonation and decarbonation stages was 50 ml/min. Multicycle performance was evaluated over 30 continuous cycles of CO₂ sorption-desorption employing the TGA program illustrated in Figure 1.

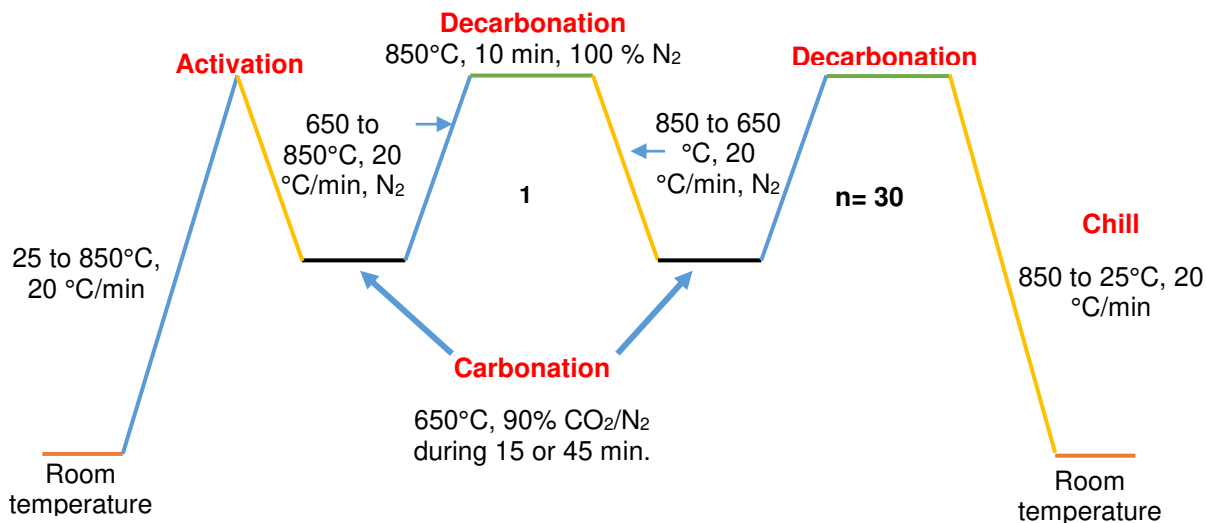


Figure 1. TGA program used for conducting uptake capacity and thermal stability (durability) in multicycle tests.

3. Results and Discussion

3.1 Characterization of sorbents

XRD diffraction experiments were initially carried out to determine the optimal preparation conditions for CaO-Saffil sorbents. The patterns for decomposition of CaAc (without Saffil) performed at 850°C for 1 h gave a mixture of CaCO₃, CaO and Ca(OH)₂, Figure 2a. Rietveld refinement analysis confirmed that the mixture comprised only ~60% CaCO₃. Increasing the calcination time to 4 h eliminated the CaCO₃ peaks, giving a mixture of CaO (~96%) and a minor amount of secondary phase (Ca(OH)₂), Figure 2b. Hence, heat-treatment at 850 °C for 4 h was adopted as the standard calcination conditions for the next trial involving CaAc impregnation of Saffil: the resulting XRD patterns showed CaO and minor peaks owing to Ca(OH)₂ plus characteristic broad peaks of δ -Al₂O₃ - the principal component of the Saffil fibres, Figure 3. The dominance of broad δ -Al₂O₃ peaks

precluded any meaningful Rietveld analysis of the XRD data from impregnated samples. However, the proportion of sorbent was determined by chemical analysis, as described below. The $\text{Ca}(\text{OH})_2$ in the various samples probably forms due to interaction with moisture from air. This effect termed air-slaking was apparent because of the high reactivity of nanometric-sized CaO formed from decomposition of CaAc , as the surface area plays an important role in the air slaking process ⁴⁵.

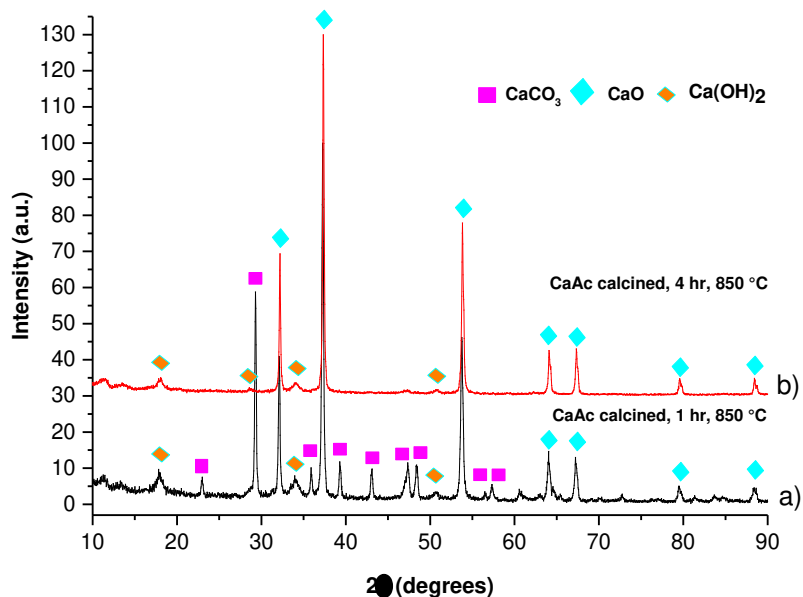


Figure 2. X-ray diffraction patterns collected from two CaAc samples which were subjected to thermal decomposition at 850°C for (a) 1 h and (b) 4 h. Phase identification was performed by reference to ICDD CaCO_3 01-080-9776, CaO 01-070-5490 and $\text{Ca}(\text{OH})_2$ 07-076-0570.

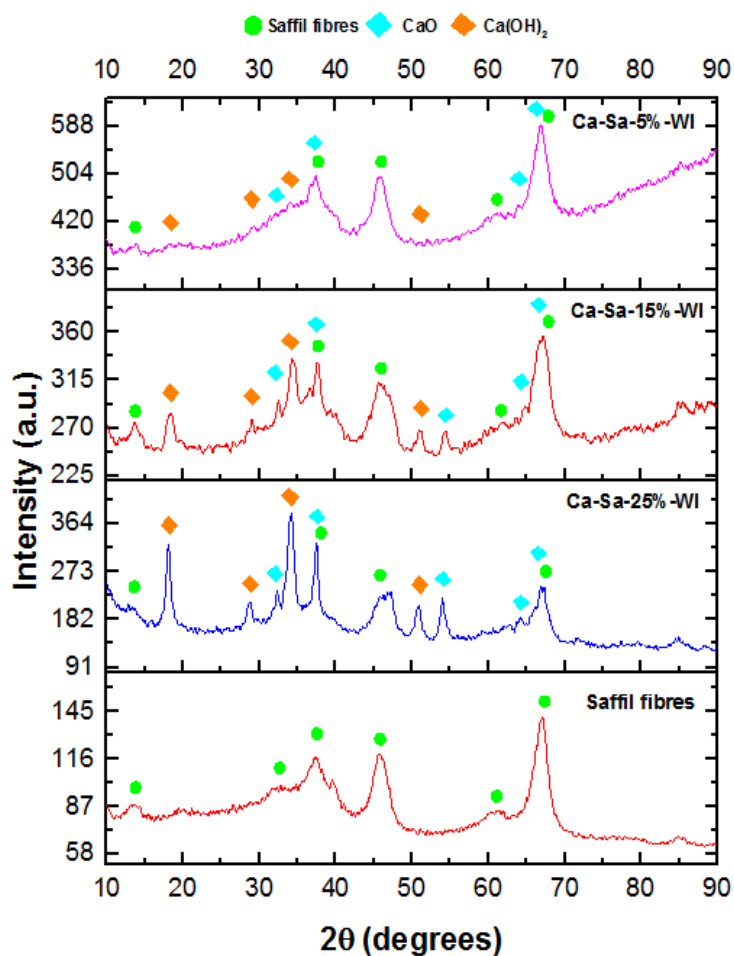


Figure 3. X-ray powder diffraction patterns of the CaO-based sorbents prepared by wet impregnation with different notional CaO contents, 5, 15, 25 wt. % and calcined at 850°C for 4 h. For comparison a Saffil fibre diffraction pattern is also shown.

The effect of solids loading and the effect of stirring during dehydration on the quality of the sorbent coating was examined using SEM, Figure 4. The vigorously stirred samples (~ 500 rpm), contained many agglomerated particles that were not attached to the support fibres, Figure 4a, whereas static conditions gave continuous coatings with fewer agglomerates, Figure 4b. Hence the static drying method was adopted throughout. The non-stirred 5 wt.% samples were of greatest uniformity-virtually all of the surface of the fibres was coated by CaO with no evidence of detached agglomerates, Figure 4c. High

magnification SEM micrographs revealed the coatings had a flake-like morphology with nanoscale dimensions. In non-stirred samples a predominantly heterogeneous nucleation process was implied by the uniformity of the sorbent coating on the Saffil substrate as evidenced from SEM-EDX mapping, Figure 4d-f.

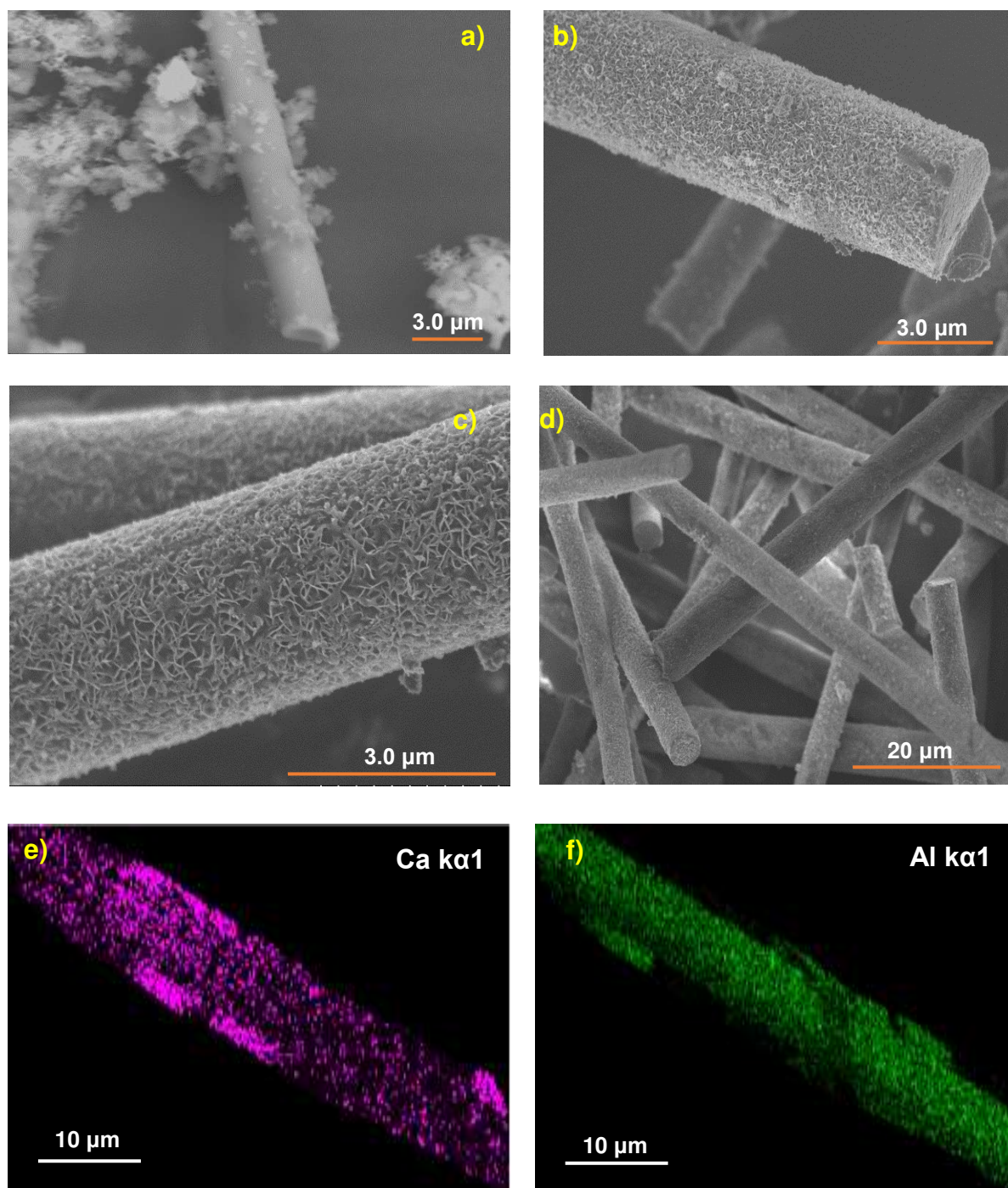


Figure 4. SEM-EDX analysis performed for the Ca-Sa-%-WI sorbents prepared in different ways: a) Ca-Sa-25%-WI sorbents under vigorous stirring (500 rpm); b) Ca-Sa-25%-WI sorbents without stirring; c) Ca-Sa-5%-WI without stirring; d) lower magnification view of Ca-Sa-25%-WI coated fibres(non-stirred); e) and f) EDX chemical mapping indicating elemental distribution of calcium and aluminium performed for Ca-Sa-25%-WI .

Quantification of the total amount of sorbent deposited on the Saffil fibres was obtained using X-ray fluorescence spectroscopy (Table 2). The amount of CaO detected in all three sorbent loadings was in reasonable agreement with the notional values (5, 15 and 25 wt. %). For simplicity of presentation, the notional 5, 15, 25 wt. % terminology is retained throughout the manuscript, but reference to Table 2 provides the accurate loadings. The composition of the uncoated fibres was found to be within 1-2 % of the values specified by the supplier, confirming the accuracy of the analytical technique.

CaO-based sorbents	CaO (%)	Al₂O₃ (%)	SiO₂ (%)
Ca-Sa-25%-WI	22.4	73.9	3.7
Ca-Sa-15%-WI	13.3	81.6	5.1
Ca-Sa-5%-WI	4.8	91.5	3.7
Saffil fibres	-	96.4	3.6

Table 2. Summary of the chemical composition in wt. % of Ca-Sa-%-WI sorbents prepared with different CaO loads (note, stated CaO content includes any CaOH₂ present).

An estimate of the thickness of the CaO coating for each of the three sample loadings was obtained from SEM observations of fibre terminations. This indicated an approximate thickness of 0.18 μm , 0.229 μm and 0.27 μm for 5, 15 and 25 wt.% CaO loadings respectively.

In terms of textural properties, the specific surface area (SSA) of the CaO-Saffil sorbents was measured using the BET method. The BET surface areas declined as the CaO content increased, which indicates the CaO coating was lower in SSA than that of the Saffil substrate. For the uncoated Saffil, the SSA was measured at $\sim 139 \text{ m}^2 \text{ g}^{-1}$, this declined in a linear manner with increasing CaO loading, reaching $\sim 92 \text{ m}^2 \text{ g}^{-1}$ for the Ca-Sa-25%-WI sample, Figure 5a. Pore size distributions and adsorption isotherms are

presented in Figure 5b and 5c respectively. Consistent with trends in the SSA data, the volume of mesopores (size range 1.5-2 nm) diminished relative to uncoated Saffil; the evolution of the type IV isotherms was consistent with the progressive coating off Saffil by the sorbent phase ^{46, 47}. The isotherms presented in Figure 5c each displayed hysteresis, with or without impregnation. However the degree of hysteresis (pore-volume width) decreased with increasing impregnation, notably for 15% and 25% CaO samples. The isotherms were of type IV with asymmetrical boundary hysteresis type H2. This type of isotherm is consistent with pore structures formed by a 3D network of cavities of different sizes connected mainly by constrictions ^{46, 47}. Cavitation processes will govern the evaporation of the physisorbed gas. The decreased width of hysteresis in the 25 wt.%, 15 wt.% and 5 wt.% with regards to uncoated Saffil fibres is associated with the filling of pores by CaO ^{48, 49}.

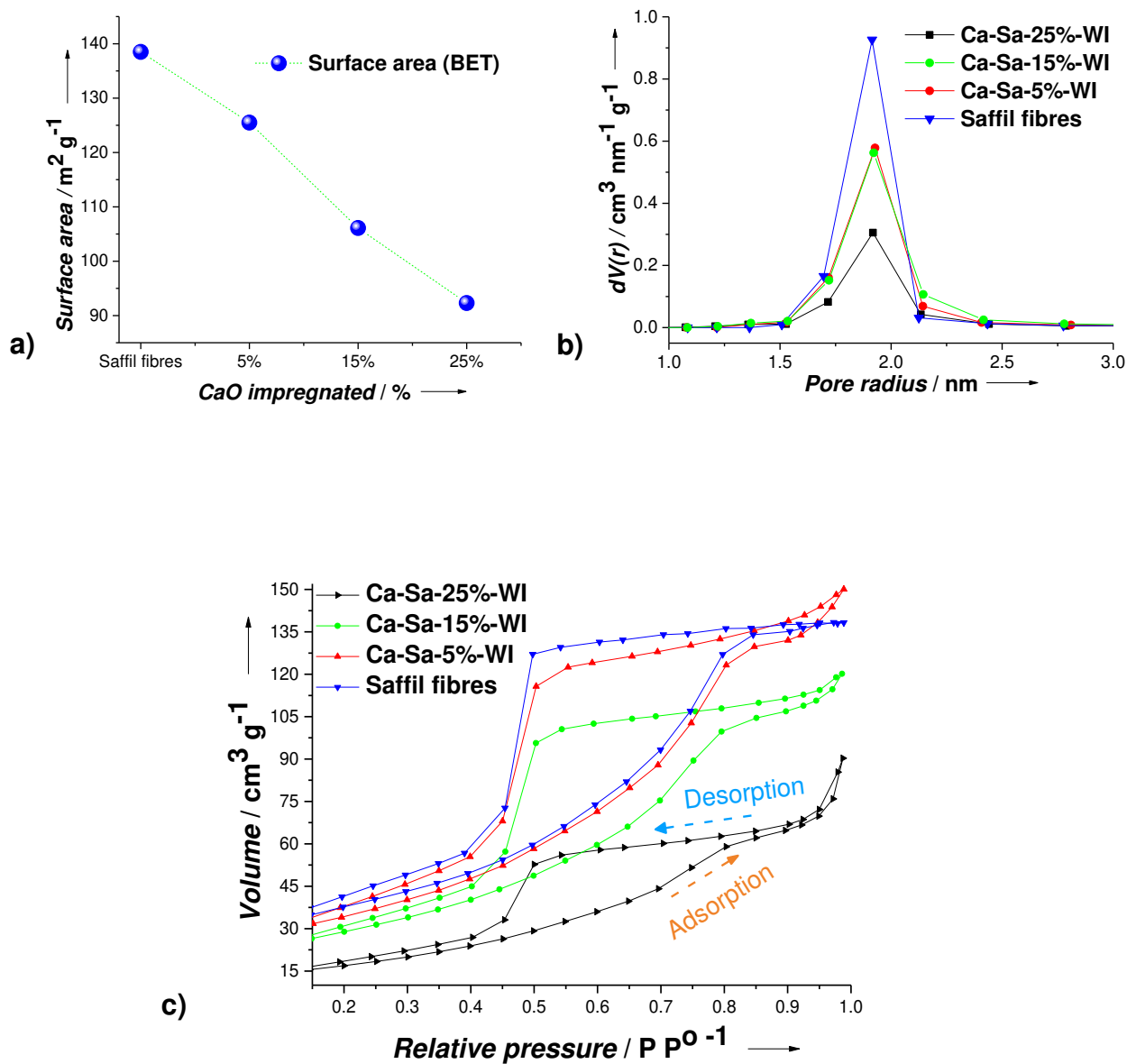


Figure 5. Textural properties evaluated for sorbents by N_2 physisorption: a) Specific surface area as a function of CaO loading, b) pore size distribution curves and c) adsorption isotherm curves for 5, 10 and 15 wt.% CaO loadings, with data also shown for as-received Saffil fibres for comparison.

3.3 CO₂ carrying capacity

Initially, the CO₂ uptake was examined by isothermal TGA at 650°C for a 45 min period using a gaseous mixture composed of 90% CO₂, balance N₂. The results shown in Figure 6 indicate that the CO₂ capture process involves two stages; a fast carbonation reaction, with a ~65% mass increase in the first 2 min, followed by a slower diffusion-controlled regime⁵⁰. The decarbonation reaction conducted at 850°C in presence of pure N₂ was rapid.

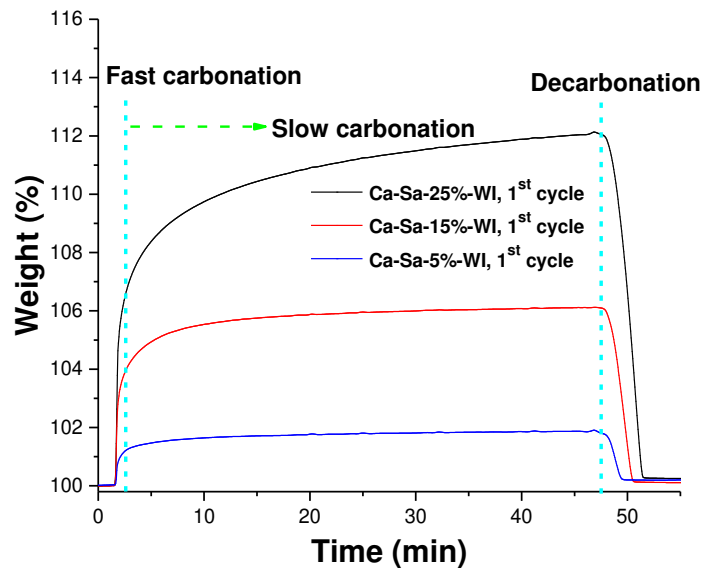


Figure 6. Isothermal carbonation profiles for the Ca-Sa-x%-WI sorbents tested by TGA (carbonation 650°C and decarbonation 850°C).

Multicycle carbonation-decarbonation TGA results are shown in Figure 7. The relative decay over 30 cycles was lowest in the Ca-Sa-5%-WI sample, albeit the carrying capacity was also lowest, as would be expected given the differing thicknesses of coatings and the additional particulate phase in the 15 and 25 wt.% samples. The carrying (CO₂ uptake) capacities in cycle 1 were 0.017 mg, 0.061 and 0.118 mg of CO₂/mg of sorbent for 5, 15 and 25 wt.% samples, respectively.

and 25 wt.% samples respectively. Bar charts representing the changes in capacity are presented in Figure 8.

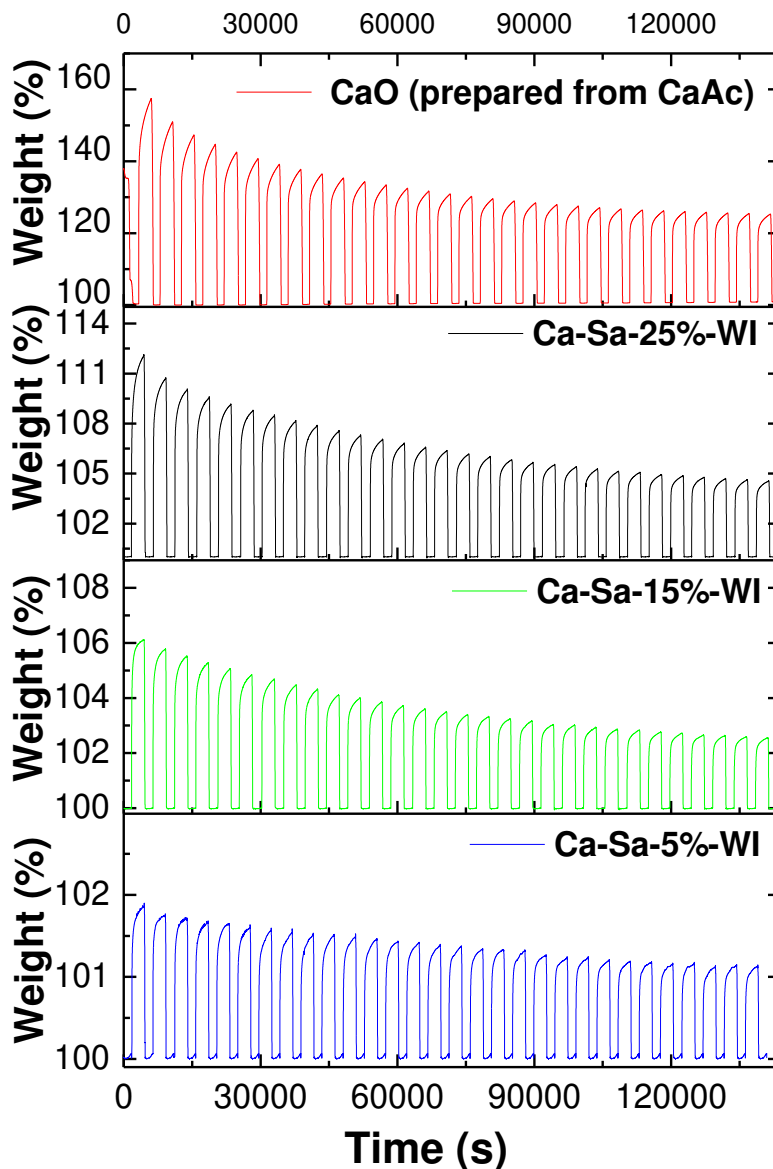


Figure 7. Carrying capacity evolution throughout 30 continuous carbonation-decarbonation cycles of Ca-Sa-%-WI sorbents impregnated with 25%, 15% and 5% of active phase and CaO prepared from CaAc. Carbonation (90 % CO₂) at 650°C in presence of a gaseous mixture composed by 90% CO₂ with N₂ as balance, whilst the decarbonation stage was carried out in pure N₂ at 850°C. Note the difference in wt.% scales for different samples.

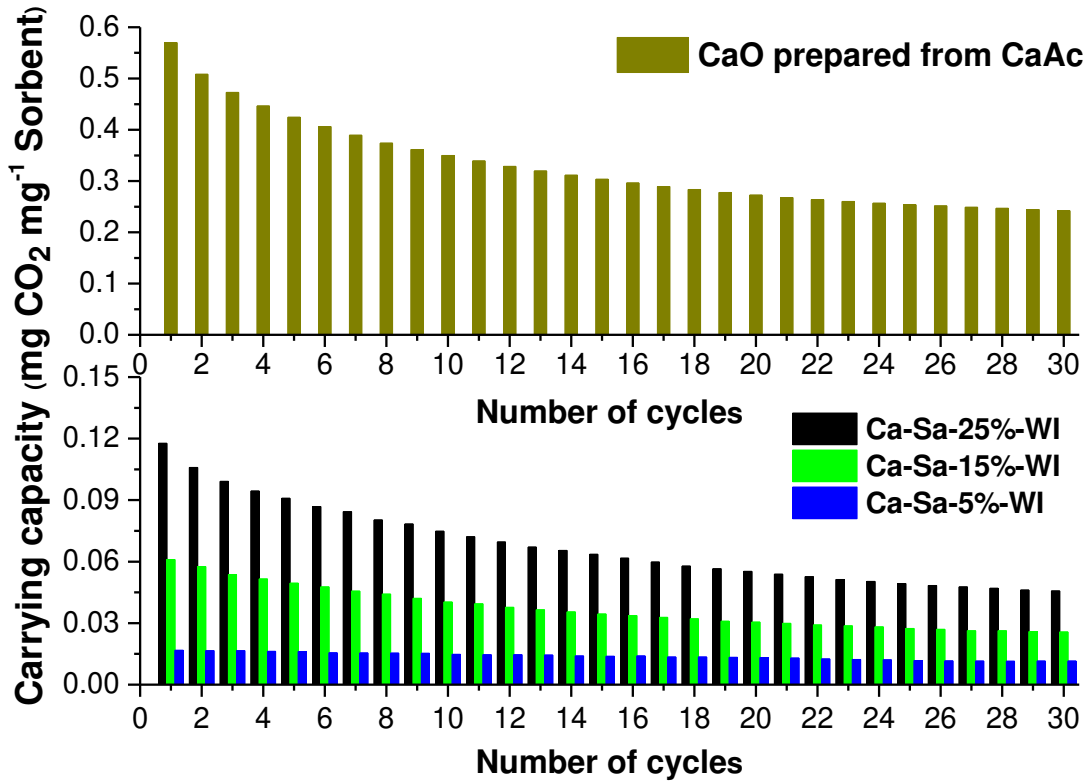


Figure 8. Carrying capacities over 30 TGA cycles of unsupported CaO (upper diagram) and Saffil supported CaO (lower diagram): (90% CO₂). Note the different capacity scale on each diagram.

The uptake capacities were calculated on the basis of equation (1) presented below.

$$CC_N = \frac{(m_{f,N} - m_i)}{m_i} \quad (1)$$

Where the subscript N represent the cycle in progress, CC_N is the maximum carrying capacity of the sorbent at cycle N , m_i is the mass of the sorbents post-activation and $m_{f,N}$ is the mass of sorbent in the course of the cycle N .

By cycle 30 around 30% of carrying capacity was lost by the Ca-Sa-5%-WI sorbent whereas the higher loadings Ca-Sa-15%-WI and Ca-Sa-25%-WI exhibited a more substantial decline in reactivity of ~50% and ~60% respectively, Figure 8. As a benchmark, multicycle TGA and carrying capacity data for a sample of calcined CaAc, produced under comparable conditions but without Saffil, are also shown in Figure 8. This illustrates there is little difference in relative decaying performance of the unsupported sorbent and the two highest loadings studied, Ca-Sa-15%-WI and Ca-Sa-25%-WI. However the lowest loading 5 wt.% sample with the thinnest coating showed greatest durability. This is attributed to the mechanical clamping effect of the substrate and the tensile forces imparted throughout the coating (anticipated to arise due to different thermal expansion coefficients of Saffil and CaO) which prevent lateral shrinkage as is documented for thin films of other ceramic materials on planar substrates⁵¹. For the thicker coatings of the 15 and 25 wt.% samples, a smaller proportion of the depth of the coating is subject to the interfacial clamping by the Saffil substrate and so volumetric densification is more pronounced after repeat carbonation-decarbonation cycles. There would also be a contribution due to densification of the free-standing agglomerates identified by SEM in these higher loadings.

In the literature, several models have been proposed to predict sorbent degradation over a large number of thermal cycles. For instance, Abanades et al. and Lysikov et al. proposed equations to determine the CaO capacity decay in recarbonation-decomposition cycles. The conversion model proposed by Abanades et al. (equation (2)) arises from a series of adaptations performed to a second-order equation for a catalyst deactivated by sintering⁵². In equation (2), X_n is the conversion at cycle N^{th} , k is the deactivation constant and X_r is the residual conversion. It must be mentioned that k is calculated by curve fitting. Moreover, Lysikov et al. rearranged the semi-empirical model suggested by Abanades et

al. and also introduced a sintering exponent n that is aimed to improve the correlation factor R^2 . As can be noticed in equation (3), the authors changed the nomenclature but the same three fitting coefficients are involved (k , n and a_∞)⁵³.

$$X_N = \frac{1}{\frac{1}{1-x_r} + kN} + x_r \quad (2)$$

$$a_N = \frac{1 - a_\infty}{(1 + kN)^n} + a_\infty \quad (3)$$

In an attempt to determine the residual carrying capacities of both Ca-Sa-25%-WI and Ca-Sa-15%-WI sorbents, equations (2) and (3) were fitted with the experimental results showed in Figure 9. From the non-linear curve fitting analysis, the R-squared values were below 0.92. Accordingly, a simple exponential-decay model coming from a first-order deactivation equation was proposed and used to correlate the experimental data. In the equation (4) that best describes the recarbonation capacity ($a_{cc,N}$) in the course of the carbonation-decarbonation cycles, the term K represent again the decay constant, a is pre-exponential factor, N is the cycle and a_r is the residual carrying capacity.

$$a_{cc,N} = a * e^{-kN} + a_r \quad (4)$$

In the curves displayed in Figure 9, dashed lines correspond to the non-linear fit performed to the experimental data. It can be discerned that there was a strong correlation between the exponential decay model and the experimental data. By using equation (4), it was possible to obtain R-squared values >0.995. According to the parameters evaluated, comparable decay constant values were obtained for the sorbents with 15 and 25 wt. %, namely, 0.0809 and 0.0816. The results apparently indicate that both sorbents exhibited very similar decay rates, as. Based on the fitting parameters, the residual carrying capacities calculated at $a_N \cong a_r$ were 0.02191 and 0.03925 mg of CO₂/mg of sorbent,

where the higher carbonation capacity belongs to the sorbent loaded with 25 wt.% of CaO. Residual reactivity in Ca-Sa-5%-WI was not modelled as the depletion trend was much less severe (Figure 8). The capture capacity was constant in 0.012 mg of CO₂/mg of sorbent between cycles 25th to 30th, and so this value corresponds to its residual reactivity.

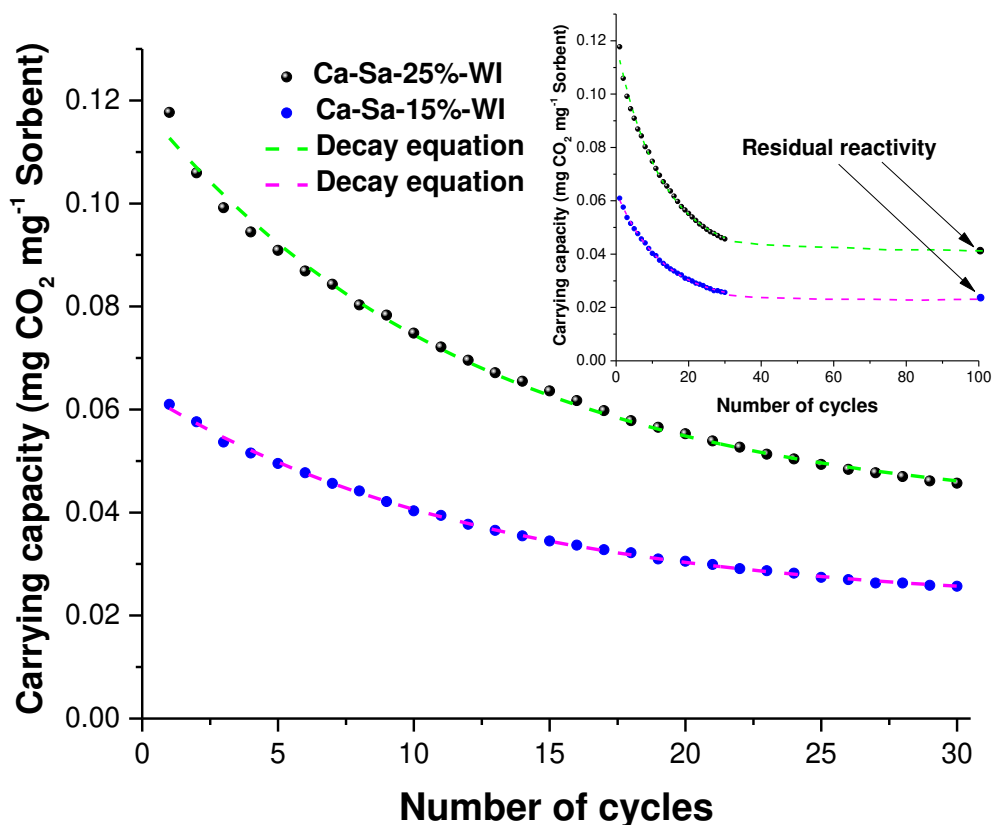


Figure 9. Residual reactivity predicted by fitting a decay model into carrying capacity curves. R-squared values >0.995 indicates that the exponential model (dashed lines) is in good agreement with experimental data.

Although CO₂ capture experiments performed with carbonation times of 45 min provided useful information on maximum CO₂ sorption capacity for Ca-Sa-%-WI sorbents, such a lengthy reaction is impractical for industrial applications. Consequently, sorbents with 15 wt % and 25 wt.% CaO were evaluated over shorter uptake periods, 15 min: the other carbonation-calcination conditions were the same as in the previous tests. Multicycle TGA

profiles presented in Figure 10 revealed capture capacities and performance losses for 30 cycles with 15 min carbonation periods similar to those observed in 45 min. This finding is consistent with the isothermal TGA data shown in Figure 6 indicating most of the uptake occurred within the first few minutes due to an initial fast carbonation associated with surface reactions. Furthermore, the sorption characteristics in 15 % CO₂ were compared to the results for 90 % CO₂ gas streams, for a 15 Figure 11. As expected, there was a decline in amount of CO₂ absorbed relative to 90 % CO₂ stream.

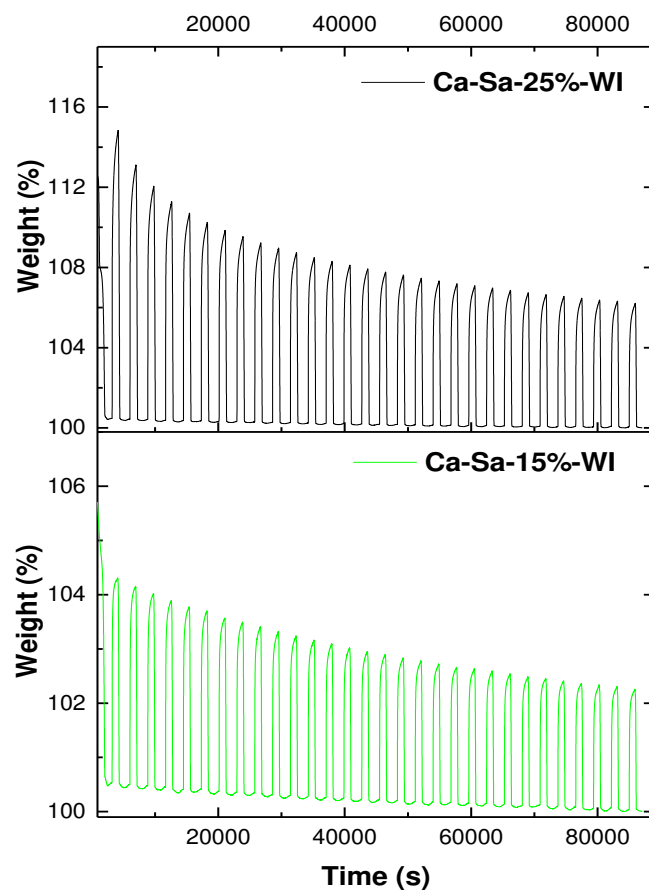


Figure 10. Multicycle CO₂ capture profiles for Ca-Sa-15%-WI and Ca-Sa-25%-WI (90% CO₂ carbonation). Carbonation-decarbonation reactions were conducted at 650°C and 850°C, respectively with a carbonation dwell time of 15 min.

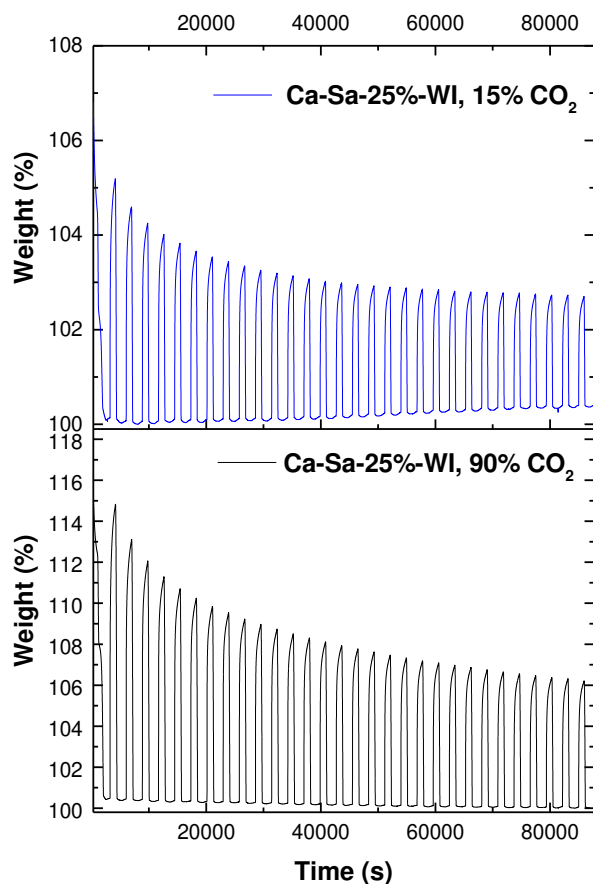


Figure 11. Comparison of 15 % CO₂ and 90 % CO₂ carbonation for Ca-Sa-25%-WI.

Carbonation and decarbonation reactions were conducted at 650°C and 850°C;
carbonation dwell times of 15 min.

On the basis of the studies carried out by various authors, natural and synthetic unsupported CaO powders tend to present a marked capture capacity depletion in the course of the first 10 cycles (>60%). This sharp decay is occasioned by sintering as described earlier^{54, 55}. However, the outcomes presented for the thinnest 5 wt.% CaO coating on Saffil revealed extended durability but at the cost of reduced initial capacity.

This sorbent retained 70% uptake capacity after 30 extended carbonation-decarbonation TGA cycles.

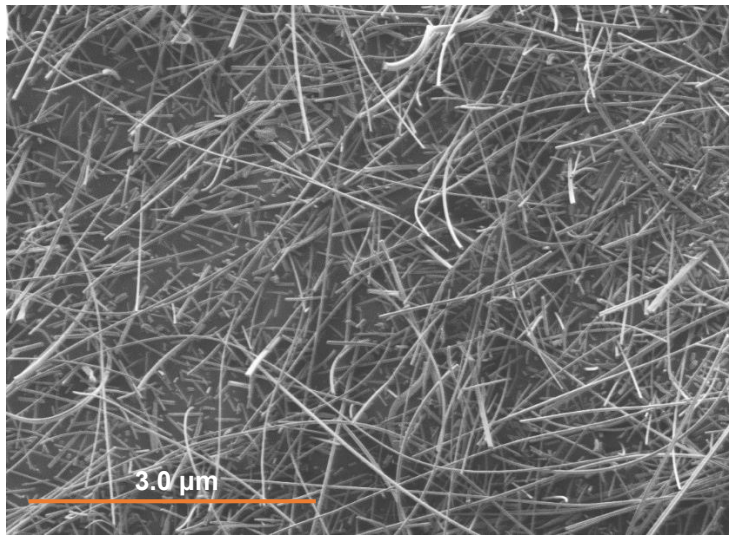


Figure 12. SEM micrograph of Ca-Sa-5%-WI sample revealing open structure of Saffil fibrous matt

The possibility of improved multicycle durability provided the motivation for selecting a fibrous low-density mat of Saffil as a sorbent support material. The concept being that the loosely entwined fibres present minimal contact between adjacent fibres onto which CaO was deposited. This open structure is illustrated in Figure 12. Thus any sintering should be restricted mainly to within an individual layer of sorbent coating. The experimental results indicate that if the coating is $< 0.2 \mu\text{m}$ in thickness (Ca-Sa-5%-WI) there is indeed little change in carrying capacity over multiple cycles (Figure 8). The thicker layers present in the higher CaO loadings are more susceptible to sintering as substrate clamping is less effective in thicker coatings (separate agglomerates may also have an effect). The disordered network of cavities in low density assemblies of Saffil fibres may have other advantages as the structure may allow a much lower pressure drop in the fixed bed reforming unit compared to other types of sorbent.

In terms of durability, one of the best performing mixed powder sorbents reported in the literature is the nano CaO/Al₂O₃ prepared through a complex solution synthesis procedure in which nano calcium carbonate, aluminium sol and hexametaphosphate are blended to form a powder composite ¹⁹. This sorbent retained 68 % of its original capacity after 50 continuous cycles in which carbonation-calcination reactions took place at 650°C and 800°C, respectively. This durability associated with the formation of a Ca₁₂Al₁₄O₃₃ co-existing phase is comparable to that of Ca-Sa-5%-WI ¹⁹. Synthetic CaO/Ca₁₂Al₁₄O₃₃ (mayenite) sorbents evaluated during 25 carbonation-calcination cycles attained capture capacities of ~0.2 mg CO₂/ mg sorbent. Their capture capacity remained stable after cycle 12: their much higher loadings of CaO (75% and 85%) allowed greater CO₂ carrying capacity than the 5-25 wt.% CaO/-Saffil sorbents in the present work ⁵⁶. Comparisons to a full range of alternative sorbents are available in references ^{57, 58}.

The simplicity of CaO/Saffil sorbent synthesis procedures, allied to the low thermal degradation of the sorbent and the possibility for future implementation as a CO₂ sorbent in SESR reactors with lower pressure drops suggest this type of fibrous substrate is worthy of further development.

4. Conclusions

Saffil fibres have been demonstrated as a new support material for CaO. The optimal synthesis parameters to load different contents of active phase (nominally 5, 15 and 25 wt.% CaO) by a wet impregnation method were determined. Microstructural analysis by scanning electron microscopy showed that CaO can be grown with a well-structured nanoflake morphology under appropriate synthesis conditions. The most favourable synthesis conditions in terms of multicycle durability were: wet infiltration of Saffil fibres without stirring; calcination at 850°C for 4h. The wt.% CaO loading produced the least degradation in multicycle TGA trials with only a ~30 % decline in CO₂ uptake capacity after 30 cycles. For 25 wt.% CaO samples the decay was ~ 60 %. The 25 wt.% sample had an initial uptake capacity of 0.118 mg CO₂/mg CaO but this declined to 0.017 mg and 0.061 mg CO₂/mg CaO for the 15 wt.% and 5 wt.% samples respectively. The improved consistency in sorbent performance of the 5 wt.% sample is attributed to the increased effects of substrate clamping and inhibition of the densification.

Acknowledgments

The Mexican National Council for Science and Technology (CONACYT) is gratefully acknowledged for providing a PhD scholarship to Sergio Ramirez-Solis and we would also like to thank the support provided by the UKCCSRC EPSRC consortium EP/K000446/1 (call 2) as well as Jonathan Cross and Adam Kelsall at Unifrax for the Saffil material. S J Milne wishes to thank Aidan Westwood for useful discussions regarding gas adsorption experiments.

References

1. Metz, B.; Davidson, O.; De Coninck, H.; Loos, M.; Meyer, L., IPCC, 2005: IPCC special report on carbon dioxide capture and storage. Prepared by Working Group III of the Intergovernmental Panel on Climate Change. *Cambridge, United Kingdom and New York, NY, USA* **2005**, 442.
2. Karami, D.; Mahinpey, N., Study of Al₂O₃ addition to synthetic Ca-based sorbents for CO₂ sorption capacity and stability in cyclic operations. *The Canadian Journal of Chemical Engineering* **2015**, 93, (1), 102-110.
3. Blamey, J.; Anthony, E. J.; Wang, J.; Fennell, P. S., The calcium looping cycle for large-scale CO₂ capture. *Progress in Energy and Combustion Science* **2010**, 36, (2), 260-279.
4. Leung, D. Y. C.; Caramanna, G.; Maroto-Valer, M. M., An overview of current status of carbon dioxide capture and storage technologies. *Renewable and Sustainable Energy Reviews* **2014**, 39, 426-443.
5. Wang, Q.; Luo, J.; Zhong, Z.; Borgna, A., CO₂ capture by solid adsorbents and their applications: current status and new trends. *Energy Environ. Sci.* **2011**, 4, (1), 42-55.
6. Jansen, D.; Gazzani, M.; Manzolini, G.; van Dijk, E.; Carbo, M., Pre-combustion CO₂ capture. *International Journal of Greenhouse Gas Control* **2015**, 40, 167-187.
7. Jiang, G.; Huang, Q.; Kenarsari, S. D.; Hu, X.; Russell, A. G.; Fan, M.; Shen, X., A new mesoporous amine-TiO₂ based pre-combustion CO₂ capture technology. *Applied Energy* **2015**, 147, 214-223.
8. Shokrollahi Yancheshmeh, M.; Radfarnia, H. R.; Iliuta, M. C., High temperature CO₂ sorbents and their application for hydrogen production by sorption enhanced steam reforming process. *Chemical Engineering Journal* **2016**, 283, 420-444.
9. Dou, B.; Wang, C.; Song, Y.; Chen, H.; Jiang, B.; Yang, M.; Xu, Y., Solid sorbents for in-situ CO₂ removal during sorption-enhanced steam reforming process: A review. *Renewable and Sustainable Energy Reviews* **2016**, 53, 536-546.
10. Kumar, S.; Saxena, S. K., A comparative study of CO₂ sorption properties for different oxides. *Materials for Renewable and Sustainable Energy* **2014**, 3, (3).
11. Duan, Y.; Luebke, D.; Henry Pennline, H., Efficient Theoretical Screening of Solid Sorbents for CO₂ Capture Applications; Capture Applications. *International Journal of Clean Coal and Energy* **2012**, 01, (01), 1-11.
12. Yong, Z.; Mata, V.; Rodrigues, A. R. E., Adsorption of carbon dioxide at high temperature—a review. *Separation and purification technology* **2002**, 26, (2-3), 195-205.
13. Molinder, R.; Comyn, T.; Hondow, N.; Parker, J.; Dupont, V., In situ X-ray diffraction of CaO based CO₂ sorbents. *Energy & Environmental Science* **2012**, 5, (10), 8958-8969.
14. Sreenivasulu, B.; Sreedhar, I.; Suresh, P.; Raghavan, K. V., Development Trends in Porous Adsorbents for Carbon Capture. *Environ Sci Technol* **2015**, 49, (21), 12641-61.
15. Memon, M. Z.; Zhao, X.; Sikarwar, V. S.; Vuppaladadiyam, A. K.; Milne, S. J.; Brown, A. P.; Li, J.; Zhao, M., Alkali metal CO₂ sorbents and the resulting metal carbonates: Potential for process intensification of Sorption-Enhanced Steam Reforming. *Environmental science & technology* **2016**, 51, (1), 12-27.
16. Ochoa-Fernandez, E.; Rusten, H. K.; Jakobsen, H. A.; Rønning, M.; Holmen, A.; Chen, D., Sorption enhanced hydrogen production by steam methane reforming using Li₂ZrO₃ as sorbent: sorption kinetics and reactor simulation. *Catalysis Today* **2005**, 106, (1-4), 41-46.
17. Puccini, M.; Seggiani, M.; Vitolo, S., Lithium silicate pellets for CO₂ capture at high temperature. *Chemical Engineering Transactions* **2013**, 35, 373-378.

18. Bamiduro, F.; Ji, G.; Brown, A. P.; Dupont, V. A.; Zhao, M.; Milne, S. J., Spray-Dried Sodium Zirconate: A Rapid Absorption Powder for CO₂ Capture with Enhanced Cyclic Stability. *ChemSusChem* **2017**, 10, (9), 2059-2067.
19. Wu, S. F.; Li, Q. H.; Kim, J. N.; Yi, K. B., Properties of a nano CaO/Al₂O₃ CO₂ sorbent. *Industrial & Engineering Chemistry Research* **2008**, 47, (1), 180-184.
20. Li, Z.-s.; Cai, N.-s.; Huang, Y.-y., Effect of preparation temperature on cyclic CO₂ capture and multiple carbonation– calcination cycles for a new Ca-based CO₂ sorbent. *Industrial & Engineering Chemistry Research* **2006**, 45, (6), 1911-1917.
21. Li, L.; King, D. L.; Nie, Z.; Howard, C., Magnesia-stabilized calcium oxide absorbents with improved durability for high temperature CO₂ capture. *Industrial & Engineering Chemistry Research* **2009**, 48, (23), 10604-10613.
22. Luo, C.; Zheng, Y.; Ding, N.; Wu, Q.; Bian, G.; Zheng, C., Development and performance of CaO/La₂O₃ sorbents during calcium looping cycles for CO₂ capture. *Industrial & Engineering Chemistry Research* **2010**, 49, (22), 11778-11784.
23. Roesch, A.; Reddy, E. P.; Smirniotis, P. G., Parametric study of Cs/CaO sorbents with respect to simulated flue gas at high temperatures. *Industrial & Engineering Chemistry Research* **2005**, 44, (16), 6485-6490.
24. Hufton, J.; Mayorga, S.; Gaffney, T.; Nataraj, S.; Rao, M.; Sircar, S. In *Sorption enhanced reaction process (SERP) for the production of hydrogen*, Proceedings of the 1998 US DOE Hydrogen Program Review, 1998; 1998; pp 693-705.
25. Fennell, P. S.; Pacciani, R.; Dennis, J. S.; Davidson, J. F.; Hayhurst, A. N., The effects of repeated cycles of calcination and carbonation on a variety of different limestones, as measured in a hot fluidized bed of sand. *Energy & Fuels* **2007**, 21, (4), 2072-2081.
26. Abanades, J. C., The maximum capture efficiency of CO₂ using a carbonation/calcination cycle of CaO/CaCO₃. *Chemical Engineering Journal* **2002**, 90, (3), 303-306.
27. Zhang, L.; Lu, Y.; Rostam-Abadi, M., Sintering of calcium oxide (CaO) during CO₂ chemisorption: a reactive molecular dynamics study. *Physical Chemistry Chemical Physics* **2012**, 14, (48), 16633-16643.
28. Park, J.; Yi, K. B., Effects of preparation method on cyclic stability and CO₂ absorption capacity of synthetic CaO–MgO absorbent for sorption-enhanced hydrogen production. *International Journal of Hydrogen Energy* **2012**, 37, (1), 95-102.
29. Wu, S.; Beum, T.; Yang, J.; Kim, J., Properties of Ca-base CO₂ sorbent using Ca(OH)₂ as precursor. *Industrial & Engineering Chemistry Research* **2007**, 46, (24), 7896-7899.
30. Kotyczka-Moranska, M.; Tomaszewicz, G.; Labojko, G., Comparison of different methods for enhancing CO₂ capture by CaO-based sorbents–review. *Physicochemical Problems of Mineral Processing* **2012**, 48, (1), 70-90.
31. Wang, J.; Huang, L.; Yang, R.; Zhang, Z.; Wu, J.; Gao, Y.; Wang, Q.; O'Hare, D.; Zhong, Z., Recent advances in solid sorbents for CO₂ capture and new development trends. *Energy & Environmental Science* **2014**, 7, (11), 3478-3518.
32. Arstad, B.; Spjelkavik, A.; Andreassen, K. A.; Lind, A.; Probst, J.; Blom, R., Studies of Ca-based high temperature sorbents for CO₂ capture. *Energy Procedia* **2013**, 37, 9-15.
33. Manovic, V.; Charland, J.-P.; Blamey, J.; Fennell, P. S.; Lu, D. Y.; Anthony, E. J., Influence of calcination conditions on carrying capacity of CaO-based sorbent in CO₂ looping cycles. *Fuel* **2009**, 88, (10), 1893-1900.
34. Lu, H.; Reddy, E. P.; Smirniotis, P. G., Calcium oxide based sorbents for capture of carbon dioxide at high temperatures. *Industrial & Engineering Chemistry Research* **2006**, 45, (11), 3944-3949.

35. Fernandez, J.; Abanades, J.; Murillo, R., Modeling of sorption enhanced steam methane reforming in an adiabatic fixed bed reactor. *Chemical Engineering Science* **2012**, *84*, 1-11.
36. Hu, Y.; Liu, W.; Sun, J.; Yang, X.; Zhou, Z.; Zhang, Y.; Xu, M., High temperature CO₂ capture on novel Yb₂O₃-supported CaO-based sorbents. *Energy & Fuels* **2016**, *30*, (8), 6606-6613.
37. Zhao, M.; Bilton, M.; Brown, A. P.; Cunliffe, A. M.; Dvininov, E.; Dupont, V.; Comyn, T. P.; Milne, S. J., Durability of CaO–CaZrO₃ sorbents for high-temperature CO₂ capture prepared by a wet chemical method. *Energy & Fuels* **2014**, *28*, (2), 1275-1283.
38. Aihara, M.; Nagai, T.; Matsushita, J.; Negishi, Y.; Ohya, H., Development of porous solid reactant for thermal-energy storage and temperature upgrade using carbonation/decarbonation reaction. *Applied Energy* **2001**, *69*, (3), 225-238.
39. Zabeti, M.; Daud, W. M. A. W.; Aroua, M. K., Optimization of the activity of CaO/Al₂O₃ catalyst for biodiesel production using response surface methodology. *Applied Catalysis A: General* **2009**, *366*, (1), 154-159.
40. Chorkendorff, I.; Niemantsverdriet, J. W., *Concepts of modern catalysis and kinetics*. John Wiley & Sons: 2017.
41. Trueba, M.; Trasatti, S. P., γ -Alumina as a Support for Catalysts: A Review of Fundamental Aspects. *European journal of inorganic chemistry* **2005**, *2005*, (17), 3393-3403.
42. Wefers, K., Alumina chemicals: science and technology handbook. *The American Ceramic Society, Westerville, Ohio* **1990**, 13.
43. Zhang, M.; Peng, Y.; Sun, Y.; Li, P.; Yu, J., Preparation of CaO–Al₂O₃ sorbent and CO₂ capture performance at high temperature. *Fuel* **2013**, *111*, 636-642.
44. Watanabe, M., Sample preparation for X-ray fluorescence analysis IV. Fusion bead method—part 1 basic principals. *English version* **2015**, 12.
45. Gallala, W.; Gaied, M.; Tlili, A.; Montacer, M., Factors influencing the reactivity of quicklime. *Construction Materials* **2008**, *161*, (1), 25.
46. Thommes, M.; Kaneko, K.; Neimark, A. V.; Olivier, J. P.; Rodriguez-Reinoso, F.; Rouquerol, J.; Sing, K. S., Physisorption of gases, with special reference to the evaluation of surface area and pore size distribution (IUPAC Technical Report). *Pure and Applied Chemistry* **2015**, *87*, (9-10), 1051-1069.
47. Song, J.; Wang, X.; Yan, J.; Yu, J.; Sun, G.; Ding, B., Soft Zr-doped TiO₂ Nanofibrous Membranes with Enhanced Photocatalytic Activity for Water Purification. *Scientific Reports* **2017**, 7.
48. Nguyen, P. T.; Fan, C.; Do, D.; Nicholson, D., On the cavitation-like pore blocking in ink-bottle pore: evolution of hysteresis loop with neck size. *The Journal of Physical Chemistry C* **2013**, *117*, (10), 5475-5484.
49. Coasne, B., Multiscale adsorption and transport in hierarchical porous materials. *New Journal of Chemistry* **2016**, *40*, (5), 4078-4094.
50. Valverde, J. M., Ca-based synthetic materials with enhanced CO₂ capture efficiency. *Journal of Materials Chemistry A* **2013**, *1*, (3), 447-468.
51. St, D.; Johansson, M., Properties of powder coatings in load carrying construction. *Journal of Coatings Technology and Research* **2005**, *2*, (6), 473-481.
52. Grasa, G. S.; Abanades, J. C., CO₂ capture capacity of CaO in long series of carbonation/calcination cycles. *Industrial & Engineering Chemistry Research* **2006**, *45*, (26), 8846-8851.
53. Lysikov, A. I.; Salanov, A. N.; Okunev, A. G., Change of CO₂ carrying capacity of CaO in isothermal recarbonation– decomposition cycles. *Industrial & Engineering Chemistry Research* **2007**, *46*, (13), 4633-4638.

54. Santos, E.; Alfonsín, C.; Chambel, A.; Fernandes, A.; Dias, A. S.; Pinheiro, C.; Ribeiro, M., Investigation of a stable synthetic sol–gel CaO sorbent for CO₂ capture. *Fuel* **2012**, 94, 624-628.
55. Valverde, J.; Perejón, A.; Perez-Maqueda, L. A., Enhancement of fast CO₂ capture by a nano-SiO₂/CaO composite at Ca-looping conditions. *Environmental science & technology* **2012**, 46, (11), 6401-6408.
56. Li, Z.-s.; Cai, N.-s.; Huang, Y.-y.; Han, H.-j., Synthesis, experimental studies, and analysis of a new calcium-based carbon dioxide absorbent. *Energy & Fuels* **2005**, 19, (4), 1447-1452.
57. Hu, Y.; Liu, W.; Chen, H.; Zhou, Z.; Wang, W.; Sun, J.; Yang, X.; Li, X.; Xu, M., Screening of inert solid supports for CaO-based sorbents for high temperature CO₂ capture. *Fuel* **2016**, 181, 199-206.
58. Salaudeen, S. A.; Acharya, B.; Dutta, A., CaO-based CO₂ sorbents: A review on screening, enhancement, cyclic stability, regeneration and kinetics modelling. *Journal of CO₂ Utilization* **2018**, 23, 179-199.